Determination of Pharmacophoric Geometry for Collagenase Inhibitors Using a Novel Computational Method and Its Verification Using Molecular Dynamics, NMR, and X-ray Crystallography

Arup K. Ghose,*[,†,‡] Margaret E. Logan,[§,∥] Adi M. Treasurywala,[†,⊥] Hsin Wang,[†] Robert C. Wahl,[†,▽] Bruce E. Tomczuk,[†,#] Madhusudhan R. Gowravaram,[†,○] Edward P. Jaeger,[†,#] and John J. Wendoloski[†,▽]

Contribution from the Sterling Winthrop Pharmaceutical Research Division, 1250 South Collegeville Road, Collegeville, Pennsylvania 19426-0900, and Life Sciences Research Laboratories, Eastman Kodak Company, Rochester, New York 14650-2158

Received July 11, 1994[⊗]

Abstract: The pharmacophoric geometry for the inhibition of human fibroblast collagenase has been determined using a novel computational method. The inhibitors used in this study, which had from seven to 11 rotatable torsion angles, did not show any irreversible movement from the pharmacophore geometry during a 20 ps room temperature molecular dynamics simulation. A parallel NMR study confirmed two torsion angles and a key atom distance, and an X-ray crystallographic study of the protein−ligand complex established the model unequivocally. The X-ray structure showed that nine out of 11 torsion angles were within the range predicted by the pharmacophoric model. For one of the two remaining torsion angles it suggested two possible values, one of which corresponded to the X-ray structure. Molecular dynamics simulations starting from the computed active conformation suggested that both of these two torsion angles could have alternate values which included the X-ray value. The computational method described here is applicable to any general molecular superimposition problem which, in rational drug design, helps: (i) to visualize the similarities among the molecules of diverse structures; (ii) to determine the active conformation for inhibiting a certain biological system, which in turn can be used for developing 3D-QSAR models; and (iii) to dock new ligands at the active site of an enzyme or a biological receptor where the conformational correspondence with the X-ray crystallographically solved ligand is not obvious. The method uses multiple distance matrices to represent the conformational flexibility and conformational diversity. The molecules may be fairly flexible, with 10−12 rotatable torsion angles. No prior assumption of active conformation is necessary during the fitting process; only a hypothesis of equivalent atoms is required to work with this method. The method suggests conformations which are within a predefined molecular mechanics energy value and indicates the possibility of multiple conformational solutions if the molecules are not sufficiently diverse or constrained.

Introduction

In traditional approaches to drug design, compounds were often tested in an animal model due to the lack of knowledge of the receptors, enzymes, and biochemical processes involving a disease state. However, in the last two decades this approach has rapidly become outdated as rational drug design has become more of a reality.[1] The operational definition of rational drug design may vary, but one common theme is the use of biological target molecules rather than animal models for the identification and optimization of lead compounds. The potency data obtained in these in vitro assays are more consistent and can be generated at a much faster pace. Advances in molecular biology and cloning techniques have made this approach even more attractive, since in some cases a large quantity of the protein can be made relatively easily. The biophysicists' view of rational drug design goes one step further. With a good supply of the enzyme, X-ray crystallographic or NMR solution of the three-dimensional structure of the enzyme−inhibitor complex has become a reality, especially when the protein is not membrane bound. These structures can be visualized in three dimensions using real time graphics. Tailoring a lead compound with substituents attractive to the neighboring groups of the biological target molecule in a cycle of structural determination is the biophysicists' perspective on rational drug design. The computational chemists want to go even further. They want to take the X-ray structure of the biological target and simulate the binding of the proposed ligands to evaluate their potential binding efficacy.[2,3] Unfortunately, the number of currently available high-resolution structures of ligand−receptor complexes is still fairly small. In order to determine the active site one needs a fairly potent inhibitor for crystallization with the enzyme or biological receptor. (The term receptor in this paper has been used to

† Sterling Winthrop.
‡ Present address: A. M. Technologies, Inc., 5 Great Valley Parkway, Suite 269, Malvern, PA 19355.
§ Eastman Kodak.
∥ Present address: Johnson and Johnson Clinical Diagnostics, Research Laboratories, 4th Floor, Building 82, RL, Rochester, NY 14650-2117.
⊥ Present address: Allelix Biopharmaceuticals Inc., 6850 Goreway Dr., Mississauga, Ontario L4V 1V7, Canada.
▽ Present address: Amgen Inc., 1840 Dehavilland Dr., Thousand Oaks, CA 91320-1789.
Present address: 3-Dimensional Pharmaceuticals, Eagle View Corporate Center, 665 Stockton Dr., Suite 104, Exton, PA 19341.
○ Present address: Affymax Research Institute, 4001 Miranda Ave., Palo Alto, CA 94304.
⊗ Abstract published in *Advance ACS Abstracts,* March 1, 1995.
(1) *Enzymes as Targets for Drug Design*; Palfreyman, M. G., McCann, P. P., Lovenberg, W., Temple, J. G., Sjoerdsma, A., Eds.; Academic Press: San Diego, 1989.
(2) Miyamoto, S.; Kollman, P. A. *Proteins: Struct., Funct., Genet.* **1993**, *16*, 226−245 and references therein.
(3) Kuntz, I. D. *Science* **1992**, *257*, 1078−1082.

0002-7863/95/1517-4671$09.00/0

represent any biological molecule with which a ligand interacts to produce a biological response.) In other words, a direct study of the interaction of the ligand with the receptor is not feasible at the early stage of drug design. To tackle this large area of drug design there are alternate approaches like pharmacophore mapping, QSAR and 3D-QSAR which allow one to rationalize existing biological efficacy data in terms of the structure of the inhibitors. In any case, a computational chemist's perspective of rational drug design is the generation of a molecule in the computer and verification of its possible biological efficacy, either using the target enzyme structure or a model of it or using a complementary model developed from the inhibitor structure, before the actual synthesis of the molecule. In spite of this, one should not forget that today the major forces of drug discovery are chemistry and biology. The objective of all these rational approaches is to utilize the chemical and biological resources most efficiently.

Most of the indirect or complementary model-building methods try to superimpose molecules so that similar groups or functionalities occupy the same region.[4,5] The identification of equivalent atoms or groups may be tricky due to the flexibility of the molecules, their structural diversity, and the established experimental fact that very similar molecules can bind to the receptor in different orientations.[6-8] Due to these difficulties, the superposition problem may be divided into the following two broad categories in which (i) atom correspondence for superposition between the reference and the test molecule has been defined and (ii) atom correspondence needs to be explored.

The flexibility of the molecules may create a few subclasses in each of the above categories: (a) Molecules are rigid. (b) The reference structure is rigid or fixed, but the test molecule is flexible. (c) Both the reference structure and the test molecule are flexible.

The complexity increases enormously as we go down along either of these subcategories. In other words, when an atom correspondence is defined in rigid molecules, it will lead to the simplest superimposition problem. When both the reference and the test molecules are flexible and the atom correspondence is to be explored, the combination will lead to the most complex superimposition problem. Earlier we dealt partially with this type of problem, by selecting a specified number of low-energy conformations of the reference molecule and using an atomic property based overlap index to measure the goodness of fit of the superimposition.[4,9] The method was found to be very useful in rationalizing certain biological activities of compounds of diverse structure.[10,11]

In this paper we will (i) describe a general method of superimposition when both the reference and the test molecules are flexible but the atom correspondence for the superimposition has been defined; (ii) apply the method to a class of human fibroblast collagenase (HFC) inhibitors to determine its bioactive conformation (pharmacophore model); (iii) run a room temperature molecular dynamics analysis to determine the stabilities of the proposed conformations; and (iv) supply NMR and X-ray data to support the derived model of the active conformation of these inhibitors.

The only major requirement for the method described herein to be applicable is that the molecules should be small enough so that an exhaustive conformational search is feasible for all of the molecules to be used in the initial experiment. A conformational search method with an efficient tree pruning algorithm[12] can easily handle up to 10 torsion angles. Unlike the ensemble distance geometry method,[13] the advantages of this method are the following:

(i) The outcome of this experiment can be monitored to set an upper limit on the molecular mechanics energy of an acceptable superimposable conformation.

(ii) When the molecules are not sufficiently diverse in their conformational behavior and therefore are superimposable in many different low-energy conformations, the method will detect such a situation and will warn the investigator about multiple possibilities. In the absence of other criteria for the acceptance of these possible conformations, one can prioritize on the basis of conformational energy.

(iii) This method also accounts for the complete low-energy conformational space and not just the grid points explored in the search process. The computational burden of this method, however, precludes its use for a fast but approximate 3D database search.[14]

Computational Methods and Experiments

Computational Background for the Identification of Superimposable Conformations in Molecules of Varied Structure. By the term "molecules of varied structure" we mean here molecules having different numbers of rotatable torsion angles between the superimposable atoms. Any computational method that wants to restrict the superposable conformations among the low-energy conformations only should have two distinct steps: (i) summarization of the low-energy conformational space and (ii) analysis of the summarized information. One can summarize the conformational space elegantly, but if the consequences of the summarization are not properly taken into account during the analysis, it may give misleading results. The conformational space is a multidimensional hyperspace; since it is never feasible to consider all points in this hyperspace, the most acceptable approach for conformational search is the grid search in which each torsion angle is varied at a specified interval, and all combinations of these grid points are evaluated energetically or sterically. The problem of this approach is that a neglected intermediate conformation may provide a better fit for the superposition on another molecule. In order to tackle this problem Crippen[15] proposed the use of the distance range matrix. Since distances are highly coordinated, one should use distance geometry embedding[16] to check the feasibility of the superimposition in a 3D Euclidean space. The conclusions drawn from the distance range matrix are valid only in an $n - 1$ dimensional space, where n is the number of atoms superimposed.[17] However, distance geometry embedding is not computationally fast enough to be applied in a large number of test cases. Another problem of embedding is that the structures obtained from simple embedding may not be energetically low.

(4) Ghose, A. K.; Crippen, G. M.; Revankar, G. R.; McKernan, P. A.; Smee, D. F.; Robins, R. K. *J. Med. Chem.* **1989**, *32*, 746-756.
(5) Barakat, M. T.; Dean, P. M. *J. Comput.-Aided Mol. Des.* **1990**, *4*, 295-316.
(6) Volz, K. W.; Matthews, D. A.; Alden, R. A.; Freer, S. T.; Hansch, C.; Kaufman, B. T.; Kraut, J. *J. Biol. Chem.* **1982**, *257*, 2528.
(7) Badger, J.; Minor, I.; Kremer, M. J.; Oliveira, M. A.; Smith, T. J.; Griffith, J. P.; Guerin, D. M. A.; Krishnaswamy, S.; Luo, M.; Rossmann, M. G.; McKinlay, M. A.; Diana, G. D.; Dutko, F. J.; Fancher, M.; Rueckert, R. R.; Heinz, B. A. *Proc. Natl. Acad. Sci. U.S.A.* **1988**, *85*, 3304.
(8) Diana, G.; Jaeger, E. P.; Peterson, M. L.; Treasurywala, A. M. *J. Comput.-Aided Mol. Des.* **1993**, *7*, 325-335.
(9) Viswanadhan, V. N.; Ghose, A. K.; Revankar, G. R.; Robins, R. K. *J. Chem. Inf. Comput. Sci.* **1989**, *29*, 163-172.
(10) Ghose, A. K.; Viswanadhan, V. N.; Sanghvi, Y. S.; Nord, L. D.; Willis, R. C.; Revankar, G. R.; Robins, R. K. *Proc. Natl. Acad. Sci.* **1989**, *86*, 8242-8246.
(11) Ghose, A. K.; Sanghvi, Y. S.; Larson, S. B.; Revankar, G. R.; Robins, R. K. *J. Am. Chem. Soc.* **1990**, *112*, 3622-3628.
(12) Lawler, E. L.; Wood, D. E. *Oper. Res.* **1966**, *14*, 669-719.
(13) Sheridan, R. P.; Nilakantan, R.; Dixon, J. S.; Venkataraghavan, R. *J. Med. Chem.* **1986**, *29*, 899-906.
(14) Clark, D. E.; Willet, P.; Kenny, P. W. *J. Mol. Graphics* **1992**, *10*, 194-204.
(15) Crippen, G. M. *J. Med. Chem.* **1979**, *22*, 988.
(16) Crippen, G. M.; Havel, T. F. *Distance Geometry and Molecular Conformation*; Research Studies Press: New York, 1988.
(17) Ghose, A. K.; Crippen, G. M. In *Comprehensive Medicinal Chemistry*; Hansch, C.; Sammes, P. G.; Taylor, J. B.; Ramsden, C. A., Eds.; Pergamon Press: Oxford, 1990; Vol. 4, pp 715-733.

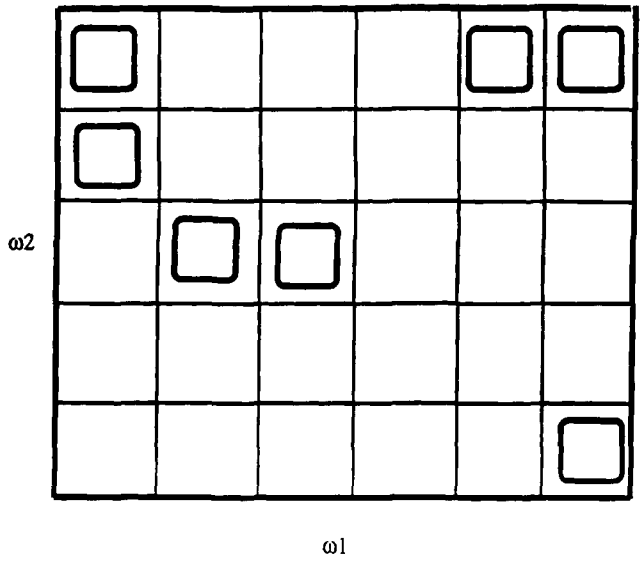

Figure 1. A schematic representation of the generation of distance matrices in the torsional space (ω's) to cover the conformations between the grids. The rectangular boxes represent the low-energy regions of the conformational space where distance range matrices are to be considered.

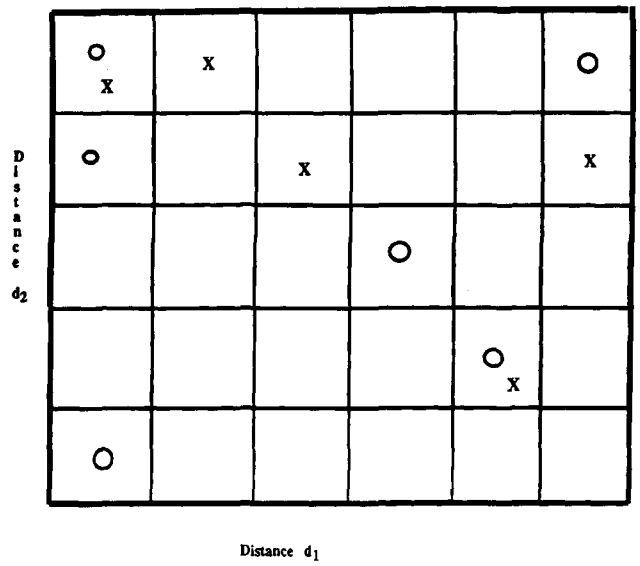

Figure 2. A schematic two-dimensional representation of an orientation map in the distance space. The circles and the crosses represent the conformations of two different molecules satisfying the distance range of the occupied grids, and d_1 and d_2 are the two pharmacophoric atom distances.

To overcome these problems Ghose and Crippen[18] proposed the construction of a distance map in the torsional space. In this approach an ensemble of distance matrices, each one representing an energetically allowed grid of the torsional space, is created (Figure 1). A distance map here may be defined as the distance range information between pharmacophoric atoms in various low-energy grids in the torsional space. If one has a hypothesis to select a few of these distance matrices as the possible pharmacophoric distances, finding overlapping energetically allowed low-energy conformations in all other molecules will suggest the availability of superimposable low-energy conformations in all molecules. In other words, the corresponding arrangement of the pharmacophoric atoms may be considered as a possible pharmacophore geometry. If one does not have any prior knowledge or hypothesis of the pharmacophoric distances, then all distance matrices should be compared. Although there are many advantages in this approach, there are two disadvantages: (i) the generation of the distance range matrices corresponding to the energetically allowed grids is somewhat inefficient; and (ii) if there are torsion angles which do not affect the location of the pharmacophoric atoms, multiple identical distance matrices along those torsional bonds will be generated.

Alternatively, one can map the torsion angles in the distance space.[19] The generation of the torsion angle map here is computationally more efficient since, once a grid size has been defined, one can very easily assign a grid to each of the energetically allowed conformations during the conformational search according to its distance property. A schematic representation of an orientation (torsional) map in the distance space is represented in Figure 2. An orientation map here can be defined as a list of grids with the following information: (i) a distance range along each distance axis of the grid and (ii) the identification number of the conformations occupying the grid. The simplest approach to test the feasibility of superimposition of a set of equivalent atoms in two molecules is to compare their orientation map. If a grid is occupied by both the molecules, those conformations are superimposable if their chirality is the same.[18]

The weakness of this approach was obvious in the present study. Here the outcome is totally dependent on the grid size. If one uses arbitrarily a very large grid size, most conformations will be placed under a few grids and will suggest many poorly superimposable conformations as superimposable.[18] Too small a grid size will create many unoccupied grids and may declare many fairly superimposable conformations as nonsuperimposable because they occupied a close neighboring grid. The ideal grid size that can avoid missing any superimposable conformations should be higher than the distance change during a torsional angle increment in the conformational search process. The distance between atoms A and D during the rotation around bond B–C (Figure 3) is given by

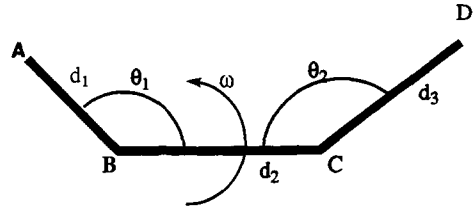

Figure 3. Description of the various internal coordinates affecting the AD distance, as used in eqs 1 and 2.

$$r^2 = d_1^2 + d_2^2 + d_3^2 - 2d_1d_2\cos\theta_1 - 2d_2d_3\cos\theta_2 + 2d_1d_3(\cos\theta_1\cos\theta_2 - \sin\theta_1\sin\theta_2\cos\omega) \quad (1)$$

where d, θ, and ω are the various bond distances and bond angles and the torsion angle, respectively. The differentiation of r^2 with respect to ω suggests

$$(\partial r^2/\partial\omega) = 2d_1d_3\sin\theta_1\sin\theta_2\sin\omega \quad (2)$$

Equation 2 shows that the change in distance between A and D depends on d_1 and d_3. The higher the value, the greater the change. In addition, the change is maximum when the bond angles as well as the torsion angle are 90°. Unfortunately, the pharmacophoric atoms A and D often are not directly bonded to B and C, and therefore all of these variables may have a wide range. In other words, the appropriate grid spacing is a function of several variables and will differ from one atom pair to another and even from one conformation to another.

The method of creating a distance map in the torsional space[18] was free from these difficulties. The distance range here tends to change according to the increment step size of the torsion angles and the other variables as shown in eq 1. The precision of the superimposed structure was determined by the coarseness of the torsional increment during the conformational analysis. However, the availability of the orientation map in the distance space[19] in the Sybyl[20] software led us to develop

(18) Ghose, A. K.; Crippen, G. M. *J. Comput. Chem.* **1985**, *6*, 350–359.

(19) Motoc, I.; Dammkoehler, R. A.; Marshall, G. R. In *Mathematical and Computational Concepts in Chemistry*; Trinajstic, N., Ed.; Ellis Horwood Ltd.: Chichester, 1986; pp 222–251.

an alternate procedure that can use the orientation map and at the same time can avoid its existing problems.

Computational Algorithm. The computational algorithm, which can be best described as the *distance hyperspace distance measurement* (DHYDM), involves the following steps:

(i) Do a conformational search and generate an orientation map (Figure 2) for each molecule independently. For the conformational analysis and orientation map generation we used the Sybyl-5.3 software.[20]

(ii) Determine the distance of the centroid of each occupied grid of molecule 1 from that of the *n*th (initially the second) molecule in the distance hyperspace using eq 3, and store the minimum distance for each grid:

$$\mathrm{ddh}_{i,j} = \sum_k (\mathrm{dc}_{i,k} - \mathrm{dc}_{j,k})^2 \qquad (3)$$

where ddh_{ij} represents the distance between the *i*th occupied grid of molecule 1 and the *j*th occupied grid of molecule 2 (or *n*) in the distance hyperspace, and $\mathrm{dc}_{i,k}$ represents the distance of the center of the *i*th grid along the *k*th distance dimension; it is simply the mean of the minimum and maximum distances of the grid along the *k*th dimension.

(iii) Increase *n* by 1. If it is less than or equal to the total number of molecules, repeat step ii. If the minimum distance is *greater* than the stored value, replace it by the current minimum. If *n* is greater than the total number of molecules, go to step iv.

(iv) Rank order the minimum distance values and accept those grids that find occupied grids within an acceptable limit.

(v) Accept the conformation in the grid if a rigid fit gives a good rms deviation of the pharmacophoric atoms from a conformation of the reference molecule in that grid.

Computational Precautions. Since distances do not keep the chirality information (enantiomeric conformations have the same distance properties), the last step of the computational algorithm may be very important. Also, Sybyl keeps many high-energy conformations in the grid at the initial stage of the conformational search, since an acceptable conformation is determined relative to the current minimum energy, and it does not go back to remove the conformations which are higher in energy than the global minimum energy conformation. One way to avoid this problem is to redo the conformational search and orientation map generation starting from the global minimum energy conformation and changing the torsion angles relative to the starting conformation.

Analysis of the orientation map was done by a Fortran program developed in house. The chirality checkup was done by actual fitting of the conformations through an SPL (Sybyl Programming Language)[20] program.

Molecular Dynamics. The purpose of this work was to run a room temperature molecular dynamics analysis for each molecule starting from the derived active conformation to determine the torsional angle range of the relevant torsion angles in the trajectory. It was expected that, if the derived conformations were too high in energy, molecular dynamics would move them away and would not bring them back.

The constant-temperature dynamics were run in Quanta 3.3.[21] Here each molecule was started from the pharmacophoric conformation and heated from 0 to 300 K in 3000 steps with a time step of 0.001 ps. It was then subjected to equilibration at 300 K in 3000 steps with a time step of 0.001 ps. Finally the structure was simulated at 300 K for 20 000 steps with a time step of 0.001 ps. Each 20 ps trajectory of the simulation part was analyzed by the analysis tools available in Quanta.

NMR Study of Protein−Ligand Complex. The recombinant truncated form of the catalytic domain of mature human fibroblast collagenase,[22,23] used for the current work, can cleave casein, gelatin, and peptide substrates but cannot cleave collagen. An HFC inhibitor labeled with [^{15}N]phenylalanine at the P_2' site (**VII**) was synthesized using α-*t*-BOC-[^{15}N]phenylalanine[24] and standard procedures.[25] A 2.1 mM collagenase sample was prepared for NMR with a slight excess of compound **VII**, in a pH 7.5 buffer containing 20 mM Tris-d_{11}, 0.2 M NaCl, 5 mM $CaCl_2$, and NaN_3. The ^{15}N-edited NOESY experiment was carried out on a Bruker AM-500 spectrometer at 35 °C. The ^{15}N-decoupling was done with a ^{15}N-180° refocusing pulse in t_1 and with GARP decoupling[26] in t_2 using a GARP decoupling device purchased from Tschudin Associates. Data were processed with FELIX-2.1 software.[27]

Results and Discussion

The method (DHYDM) was applied to a set of six partially constrained and unconstrained inhibitors of human fibroblast collagenase (HFC) (Figure 4). Human fibroblast collagenase (HFC) is a member of a family of calcium dependent zinc endoproteinases which are often termed matrix metalloproteinases (MMPs).[28−31] HFC is responsible for the cleavage of collagen, a major component of cartilage. Blocking the activation of these MMPs is considered to be a potential strategy to prevent tissue damage. The computational and NMR works described in this paper were done in parallel and were completed more than a year before[32] the X-ray crystallographic structure was solved.[22]

Pharmacophoric Atom Selection. The pharmacophore atom selection for the present work was based on the structure−activity relationships (SAR) studies reported in the literature.[28,30] It was known that HFC inhibitors should have the following structural features (see Figure 5):

(i) *A zinc ligand at the scissile peptide bond.* Replacement of the scissile peptide bond by groups able to act as zinc ligands is the basic approach that has been used in the design of collagenase inhibitors. The hydroxamate functionality is a very effective scissile bond surrogate in collagenase inhibitors.[28,30] Other zinc ligands, like thiol, carboxylate, and phosphonate, also serve this function effectively. We used only hydroxamates in this modeling study because the other ligands have different coordination geometry around Zn. Since Zn was not parametrized in the Sybyl software, a dummy atom was used in its place as one of the pharmacophoric atoms. The thermolysin−hydroxamate complex X-ray structure[33] was used for this placement.

(ii) *A hydrophobic group on the P_1' amino acid.* It was known that the complete removal of the isobutyl group led to a remarkable decrease in binding affinity. Decreasing the size to *n*-propyl led to a very small decrease in affinity.[28] This SAR indicated the necessity of one of the terminal methyl groups for the activity; to avoid the computational complications arising from the stereochemical difference of the two terminal methyl

(20) Tripos Associates Inc., 1699 S. Hanley Rd., St. Louis, MO 63144.
(21) Molecular Simulations Inc., 200 Fifth Avenue, Waltham, MA 02154.
(22) Spurlino, J. C.; Smallwood, A. M.; Carlton, D. D.; Banks, T. M.; Vavra, K. J.; Johnson, J. S.; Cook, E. R.; Falvo, J.; Wahl, R. C.; Pulvino, T. A.; Wendoloski, J. J.; Smith, D. L. *Proteins: Struct., Funct., Genet.*, in press.
(23) Murphy, G.; Allan, J. A.; Willenbrock, F.; Cockett, M. I.; O'Connell, J. P.; Docherty, A. J. P. *J. Biol. Chem.* **1992**, *267*, 9612−9618.
(24) Cambridge Isotope Laboratories, 20 Commerce Way, Woburn, MA 01801.
(25) Dickens, J. P.; Donald, D. K.; Kneen, G.; Mckay, W. R. *Eur. Pat.* 214639, 1987.
(26) Shaka, A. J.; Baker, P. B.; Freeman, R. *J. Magn. Reson.* **1985**, *64*, 547.
(27) Biosym Technologies Inc., 9685 Scranton Road, San Diego, CA 92121−2777.
(28) Johnson, W. H.; Roberts, N. A.; Borkakoti, N. *J. Enzyme Inhib.* **1987**, *2*, 1−22.
(29) Wahl, R. C.; Dunlap, R. P.; Morgan, B. A. *Annu. Rep. Med. Chem.* **1989**, *25*, 177−184.
(30) Schwartz, M. A.; Van Wart, H. E. *Prog. Med. Chem.* **1992**, *29*, 271−334.
(31) Beszant, B.; Bird, J.; Gaster, L. M.; Harper, G. P.; Hughes, I.; Karran, E. H.; Markwell, R. E.; Miles-Williams, A. J.; Smith, S. A. *J. Med. Chem.* **1993**, *36*, 4030−4039.
(32) A part of the computational method and results were presented in the Molecular Graphic Society Annual Meeting, May 15−19, 1992, Bath, England.
(33) Matthews, B. T. *Acc. Chem. Res.* **1988**, *21*, 333−340.

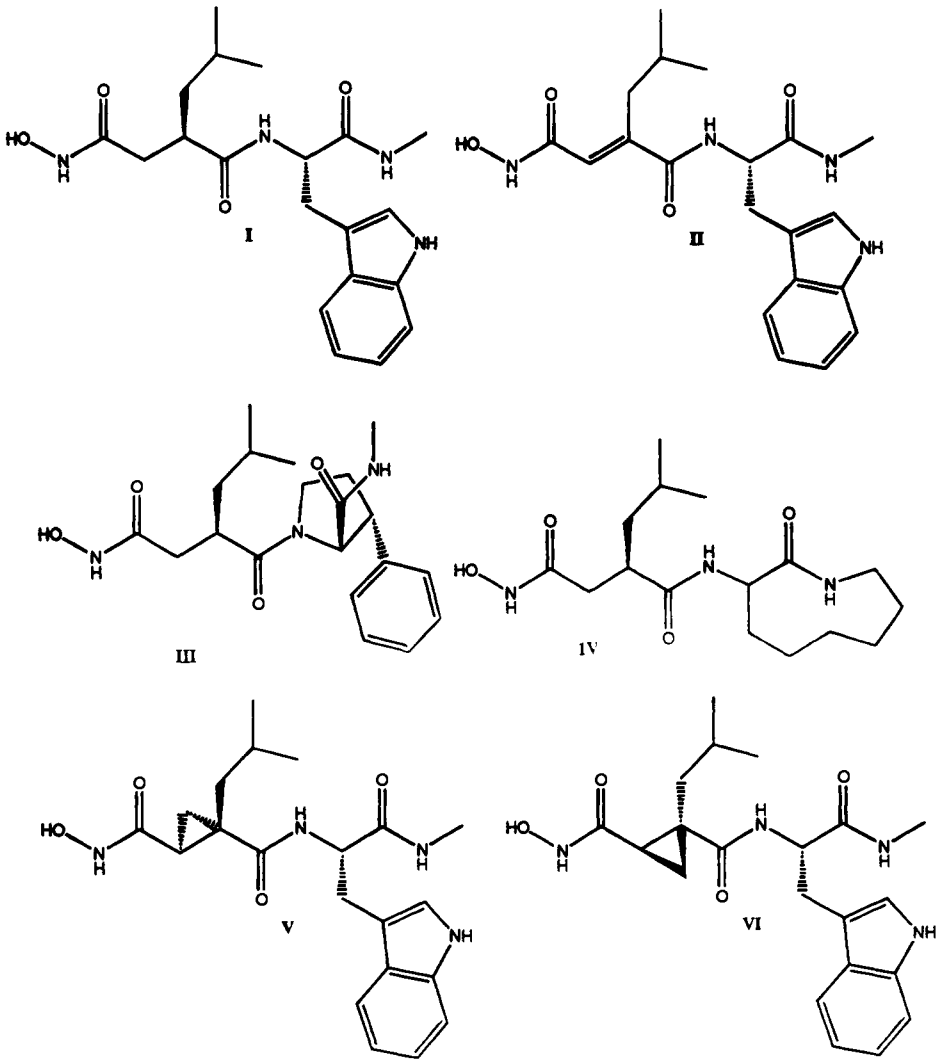

Figure 4. Various constrained and unconstrained inhibitors used in the current analysis.

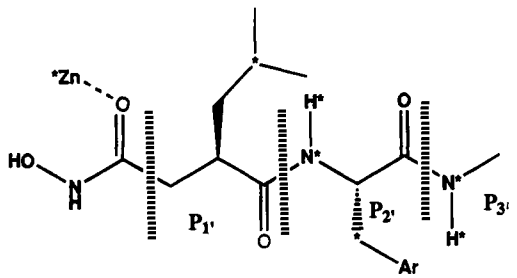

Figure 5. The various atoms used as pharmacophoric atoms in accordance with SAR data.

groups we selected the second carbon as one of the pharmacophoric atoms.

(iii) *A hydrogen bond donor at the $P_1'-P_2'$.* Replacement of the $P_1'-P_2'$ amide linkage (−CONH−) by an ester (−COO−) or a retroamide (−NCHO−) led to inactive compounds.

(iv) *A hydrogen bond donor at the $P_2'-P_3'$.* Replacement of the $P_2'-P_3'$ amide (−CONH−) as in iii led to a considerable decrease in binding affinity. Two pharmacophoric atoms were used to represent each of these hydrogen donors to keep the directionality of hydrogen bond donation.

(v) *A hydrophobic alkyl or aralkyl group at the P_2' side chain.* This increased the binding affinity considerably. Ala at P_2', for example, showed considerably less potency.[28] This structure–activity data led us to select the seven atoms as critical pharmacophoric atoms (Figure 5).

Table 1. Binding Affinity (K_i) Values of the Various Inhibitors for Human Fibroblast Collagenase

compd	K_i values (μM)
I	0.002
II	0.13
III	0.31
IV	0.100[a]
V (or **VI**)[b]	0.77
VI (or **V**)[b]	0.81
V, VI (1:1)	0.72

[a] K_i from Johnson et al., ref 28. [b] The stereochemical correspondence of these compounds has not been determined. The structures **V** and **VI** are marked only to illustrate the computational results.

Inhibitor Selection. Selection of the inhibitors for this study (Figure 4) was based on structure and potency (Table 1). **I** is a very potent but unconstrained inhibitor of HFC.[34] In olefin **II**[35,36] the ϕ_1' angle is constrained to 180° while in the P_2' proline derivative **III**[37] the ϕ_2' angle is constrained to approximately −75°. The activity of the lactams of type **IV** was found to be a function of the number of CH_2 groups connecting the Cα and N.[28] For the 7-membered lactam both the S and R isomers have activities in the micromolar range, but as the ring size was increased from nine to 13 the HFC inhibition also increased.

(34) Dickens, J. P.; Donald, D. K.; Kneen, G.; Mckay, W. R. U.S. Patent 4599361, 1986.
(35) Logan, M. E.; Seelye, J. A.; Wahl, R. C. Unpublished result.
(36) Galardy, R. E.; Grobelny, D. U.S. Patent 05189178, 1993.
(37) Goswami, R.; McGarry, R. Private communication.

Table 2. Computational Aspects of Conformational Analysis of the Various Inhibitors

molecule	no. of rotating bonds	no. of conformations generated[a]	CPU time (days:h:min)[b]
I	11	30095	07:09:03
II	10	69577	00:17:56
III	9	118	00:00:16
IV	7	3286	00:00:37
V	10	833	00:00:04
VI	10	4462	00:00:28

[a] The theoretical number of conformations in most cases is astronomically large, but most of these conformations are rejected on the basis of van der Waals penetration or on the basis of the energy window selected during conformational analysis. [b] A single-processor Sun 490 server was used for this calculation.

Table 3. Backbone Torsion Angles of the Minimum Energy Conformation of the Various Molecules as Obtained from the Combinatorial Conformational Search Followed by Minimization

	torsion angles[a] (deg)						
molecule	p−ω	p−ϕ_1'	ψ_1'	ω_1'	ϕ_2'	ψ_2'	ω_2'
I	85.2	−58.7	−68.6	−176.4	−82.1	66.6	−179.6
II	157.0	175.8	139.4	178.2	−147.2	55.0	−179.6
III	73.4	−178.6	93.0	−179.0	−79.1	71.5	178.2
IV	−77.1	72.7	79.1	178.8	−162.5	−66.3	−168.0
V	−80.8	141.5	−78.5	177.0	−73.8	152.4	−179.3
VI	−125.4	−141.4	72.0	175.0	−68.0	−40.7	178.0

[a] See Figure 6 for a more detailed description of the torsion angles.

Table 4. Side Chain Torsion Angles in the Minimum Energy Conformation of the Various Molecules as Obtained from the Combinatorial Conformational Search Followed by Minimization

	torsion angles[a] (deg)				
molecule	χ_{11}	χ_{12}	χ_{12}'	χ_{21}	χ_{22}
I	170.9	−179.6	57.9	−53.6	111.6
II	−63.6	173.5	−63.9	−57.8	−92.3
III	173.6	177.4	54.7	−83.1	−156.5
IV	−160.4	177.2	−60.2		
V	−167.4	−177.3	60.3	−178.7	95.6
VI	164.1	175.6	−61.7	66.3	−98.3

[a] See Figure 6 for a more detailed description of the torsion angles.

The potencies parallel the amount of trans amide conformation in the lactams. The nine-membered-ring lactam, the smallest and conformationally most simple of the cyclic lactams containing a trans amide bond, was selected here. When this modeling experiment was performed, only a mixture of the two diastereomers **V** and **VI** had been synthesized.[35] Accordingly, two superimposition experiments were done, in which molecules **I**−**V** were used in one and **I**−**IV** and **VI** in the other. The hope was that only one structure would be superimposable, allowing an indirect determination of the stereochemistry of the active diastereomer. Since the HFC K_i's of the constrained compounds **II**−**VI** were somewhat higher than that of the unconstrained compound **I**, one may question whether all of the pharmacophoric groups in the constrained compounds could reach the corresponding enzyme site pockets. However, most often complete removal of these pharmacophoric groups led to a far greater decrease in binding affinity. This prompted us to believe that all the pharmacophoric groups are roughly reaching the corresponding active site pocket in constrained inhibitors **II**−**VI**.

Molecule Building and Conformational Analysis. Except for molecule **IV**, all the structures were generated from the standard fragment library of the Sybyl software. For molecule **IV** a Cambridge Structural Database (CSD)[38] search was conducted for nine-membered lactams. Only the structures having trans amide bonds were considered as possible candidates. Two substituted monocyclic systems, AZCNOO and CAPRYL, and one tricyclic system, BOVYIU, were selected in this process. These structures were stripped of their substituents or extra rings and minimized with Gasteiger−Mersilli atomic charges[39a] and a distance-dependent dielectric constant ($D = r$). The energy of the three minimized nine-membered lactam structures were within 0.5 kcal/mol, CAPRYL being most stable. These structures differed in ring pucker also. We arbitrarily selected BOVYIU as the initial structure for our calculation. All of the molecules were subjected to a geometry optimization before any conformational search. After minimization a dummy atom was generated, mimicking the geometry of hydroxamate−Zn complexes in thermolysin[33] due to the lack of molecular mechanics parameters in the Sybyl force field.

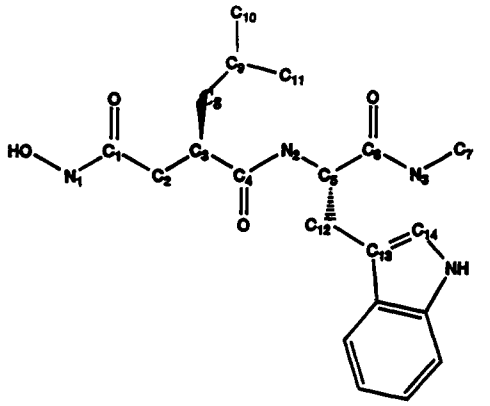

Figure 6. Description of the various torsional angles: p−ω = N_1−C_1−C_2−C_3; ϕ_1' = C_1−C_2−C_3−C_4; ψ_1' = C_2−C_3−C_4−N_2; ω_1' = C_3−C_4−N_2−C_5; ϕ_2' = C_4−N_2−C_5−C_6; ψ_2' = N_2−C_5−C_6−N_3; ω_2' = C_5−C_6−N_3−C_7; χ_{11} = C_2−C_3−C_8−C_9; χ_{12} = C_3−C_8−C_9−C_{10}; χ_{21} = N_2−C_5−C_{12}−C_{13}; χ_{22} = C_5−C_{12}−C_{13}−C_{14}.

During the conformational analysis, the acyclic torsion angles of each inhibitors were rotated from 0 to 359° at an interval of 30°; cyclic torsion angles were held fixed, and so were the terminal methyl groups. In the initial study, the standard pharmacophore modeling method was applied, in which one starts from a molecule and creates an orientation map (Figure 2) of the pharmacophoric atoms during the conformational analysis. For the next molecule one uses the previously generated orientation map and creates a new map during its conformational search. This approach is very fast because it considers only the conformations that have distances overlapping the occupied grids of the previously generated distance map. However, its problem is that the relative stability of the conformation of the second and subsequent molecules is unknown in the absence of the energy of the global minimum energy conformation. The global minimum energy conformation or the grid point closest to it may get excluded due to the distance constraints on the pharmacophoric atoms. Even when we neglected this problem, this method failed to give any distance grid that could be occupied by all the molecules used in the current study. This led us to apply the modified computational procedure (DHYDM) as described in the method section. The computational time required and the number of conformations generated during the conformational analysis of these medium-sized molecules is summarized in Table 2. These values will also explain the necessity of the alternate procedure. From the CPU time it is obvious that neither decreasing the

(38) Cambridge Crystallographic Data Center, 12 Union Rd., Cambridge CB2 1EZ, U.K.

(39) (a) Gasteiger, J.; Marsili, M. *Tetrahedron* **1980**, *36*, 3219−3288. (b) Ghose, A. K.; Jaeger, E. P.; Kwalczyk, P. J.; Peterson, M. L.; Treasurywala, A. M. *J. Comput. Chem.* **1993**, *14*, 1050−1065.

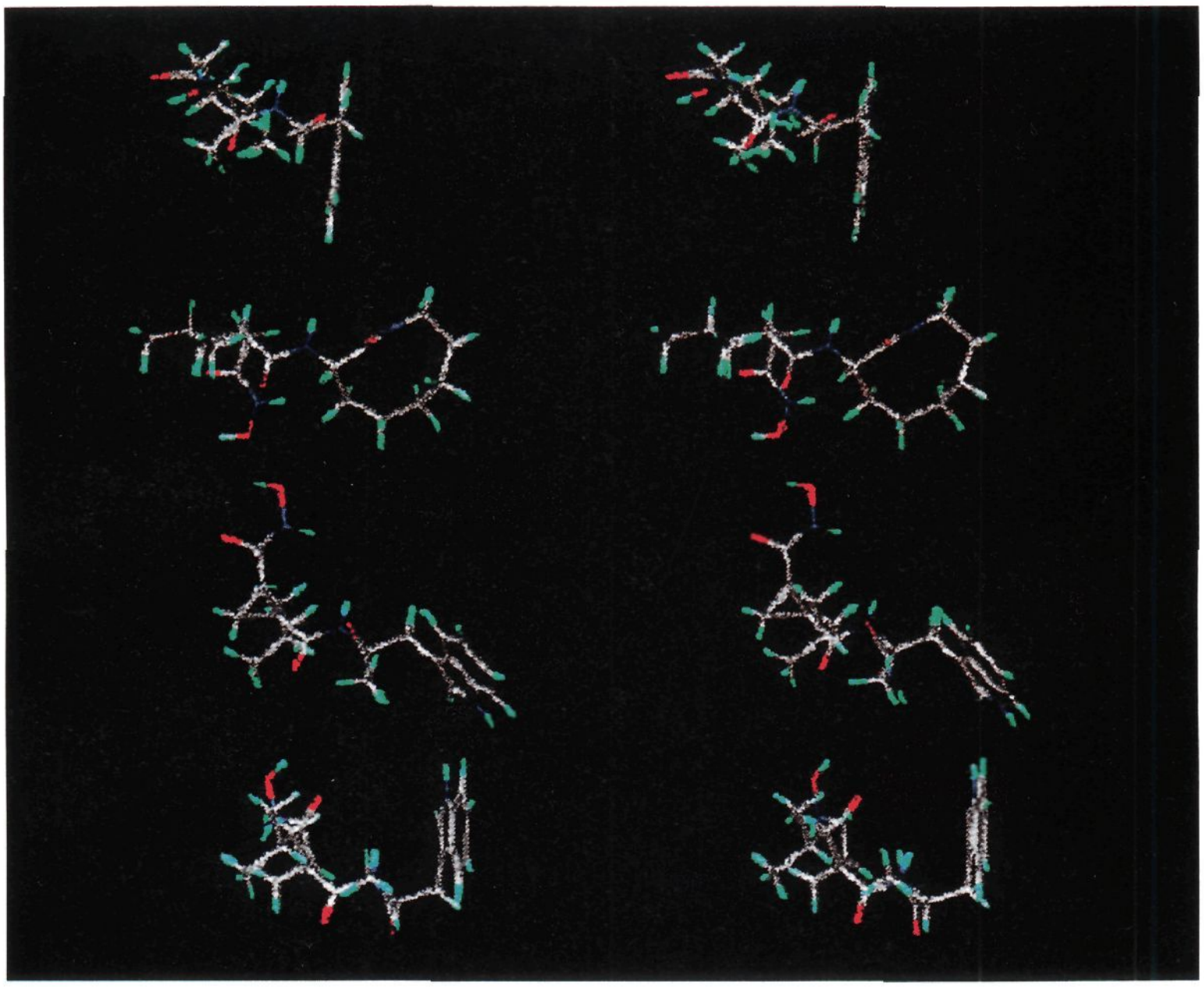

Figure 7. The relaxed stereo picture of the minimum energy conformations of **I**, **IV**, **V**, and **VI** (from top to bottom).

step size of the angle increment nor repeating the conformational search by gradually increasing the distance grid size is possible for a problem of this size. The number of conformations generated in the conformational search is considerably less than the theoretical number of conformations arising from the combinations of possible conformations. This is the consequence of two factors: (i) neglect of sterically disallowed conformations and (ii) neglect of energetically disallowed conformations. The three allowed van der Waals overlapping factors used for this study were 0.85 of the sum of the van der Waals radii for 1,5 and higher membered atoms, 0.80 for the 1,4 membered atoms, and 0.65 for hydrogen-bonding atoms. The energy cutoff value for accepting a conformation was selected to be 5 kcal/mol. All torsion angles were initially set to 0°.

Since a full conformational search was done for each molecule in the current method, it may be worthwhile to compare the minimum energy conformations of these peptide-like molecules (especially the P_2' region) with the available experimental and theoretical results. We have previously shown that the Tripos force field gave a reasonable result during conformational analysis when applied to a set of representative organic molecules.[39b] If we concentrate on the acyclic P_2' compounds (**I**, **II**, **V**, and **VI**), we can see that the ϕ_2 and ψ_2 angles (Table 3) of the four minima belonged to four different types. Consideration of the *derivation diagram* of the Ramachandran plot[40,41] shows that all four belonged to the region where all residues are allowed. The ϕ_2 angle of both the cyclic compounds **III** and **IV** is constrained in a ring and is therefore determined by the ring conformation. The ψ_2 angle is also a part of the ring conformation in **IV**. Despite these complications, the ϕ_2 and ψ_2 angles in these compounds were in the region of the Ramachandran plots in which all amino acid residues have allowed conformations. The ω angles were all trans. Since none of the test compounds had true amino acid residues at P_1', no effort was made to analyze their torsion angles in terms of regular peptide torsion angles. The side chain torsion angles (χ_{21}, χ_{22}, see Table 4) at the P_2' position of the four acyclic peptides (**I**, **II**, **V**, and **VI**) had four different sets of angles. However, each torsion set value was consistent with the library of torsion angles of tryptophan (Trp) as reported by Ponder et al.[42] Stereo pictures of the minimum energy conformations of these four P_2' acyclic peptides are shown in Figure 7.

Torsion Mapping and Pharmacophore Geometry Determination. The orientation map (Figure 2) was created independently for each molecule with a distance grid size of 0.6 Å. In the first experiment molecules **I**−**V** were used. Although the combinatorial nature of this analysis makes the final outcome independent of the order of use of the various molecules, in our analysis we started with **IV** and ended with **I**. The complete analysis of the orientation maps took less than 15 min. The maximum distance of the closest occupied grid for the rest of the molecules in the distance hyperspace was at 1.90 Å. Except for **IV**, the starting molecule of the DHYDM analysis, an acceptable neighboring grid often contained many conformations. Also several grids were often at the same acceptable

(40) Mandel, N.; Mandel, G.; Trus, B. L.; Rosenberg, J.; Carlson, G.; Dickerson, R. E. *J. Biol. Chem.* **1977**, *252*, 4619−4636.
(41) Richardson, J. S. *Adv. Protein Chem.* **1981**, *34*, 167−339.
(42) Ponder, J. W.; Richards, F. M. *J. Mol. Biol.* **1987**, *193*, 775−791.

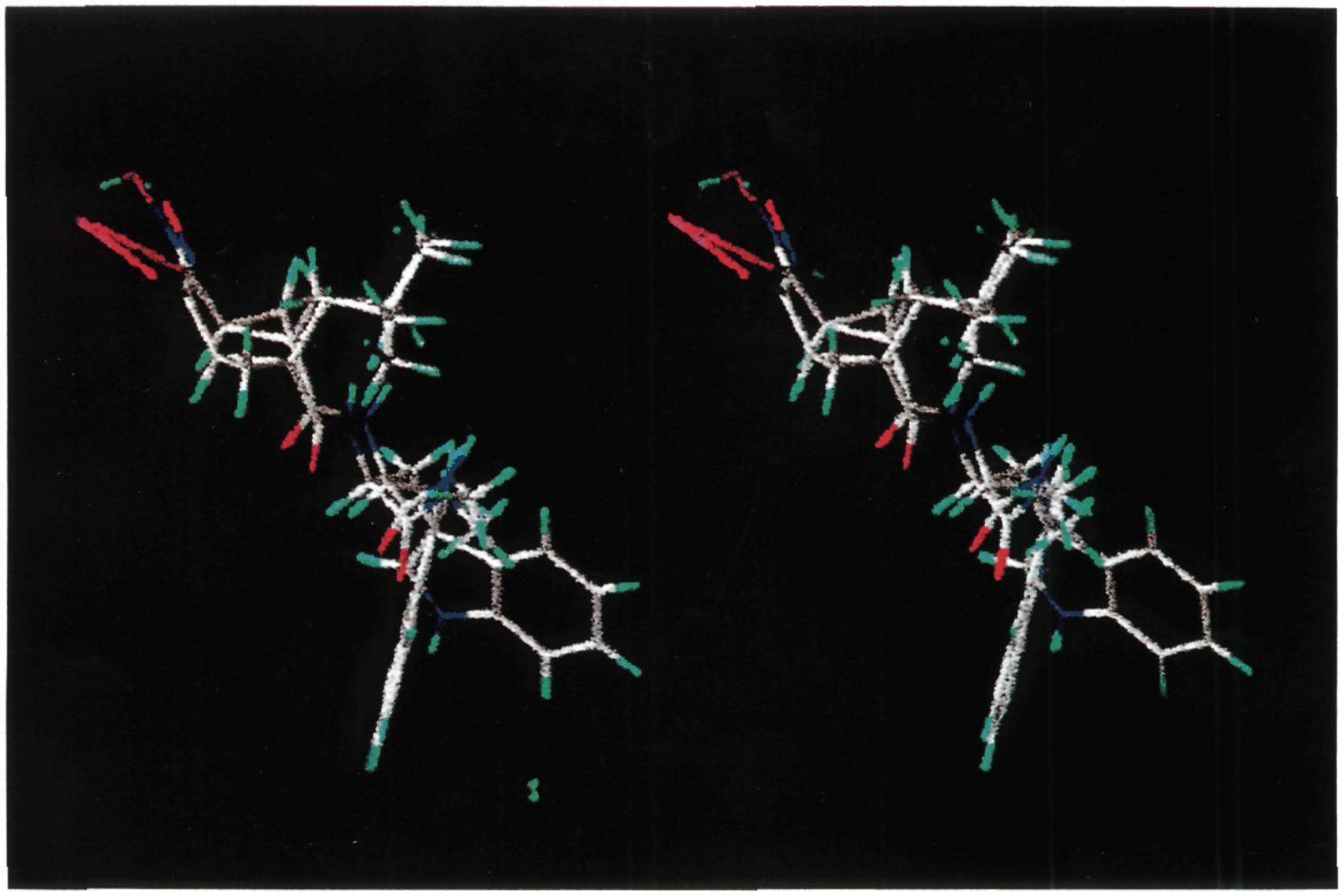

Figure 8. The relaxed stereo picture of the active conformations of **V** and **VI** in two experiments.

Table 5. Backbone Angles in the Superimposed Conformation from Molecules **I**−**V**

	torsion angles[a] (deg)						
molecule	p−ω	p−ϕ_1'	ψ_1'	ω_1'	ϕ_2'	ψ_2'[b]	ω_2'
I	103.3	160.8	119.1	−179.1	−58.2	−54.7	−179.7
II	129.6	178.3	122.5	177.1	−58.7	−59.3	−178.8
III	91.2	172.7	89.5	−175.3	−73.9	−28.3	179.4
IV	104.8	164.8	148.1	177.3	−84.0	−61.4	−167.7
V	123.6	153.5	119.1	178.4	−60.9	−60.7	−177.8

[a] See Figure 6 for a more detailed description of the torsion angles. [b] Another value (150°) around this torsion angle was also consistent with all these inhibitors; see text for detailed discussion.

Table 6. Side Chain Angles in the Superimposed Conformations from Molecules **I**−**V**

	torsion angles[a] (deg)				
molecule	χ_{11}	χ_{12}	χ_{12}'	χ_{21}	χ_{22}
I	178.2	−178.8	59.6	−179.7	89.8
II	174.2	173.7	−64.7	−59.0	116.5
III	169.1	176.6	54.2	−97.4	52.0
IV	176.5	−157.8	80.3	(−75.6)	
V	−175.5	146.2	−91.1	−117.3	118.7

[a] See Figure 6 for a more detailed description of the torsion angles.

distance. Many of these conformations did not superimpose on the starting molecule due to opposite chirality (see Computational Methods and Experiments section for greater detail). The rms fit of the pharmacophoric atoms was used to select the conformation uniquely. The backbone and side chain torsion angles of the superimposed conformations thus obtained are shown in Tables 5 and 6.

Repetition of the same experiment with molecules **I**−**IV** and **VI** produced the second set of conformations as given in Tables 7 and 8. Comparison of the two sets of conformations suggested that they are practically identical. The stereo picture of the pharmacophoric conformations of diastereomers **V** and **VI** obtained in these two experiments is shown in Figure 8.

Table 7. Backbone Angles of the Superimposed Conformation from Molecules **I**−**IV** and **VI**

	torsion angles[a] (deg)						
molecule	p−ω	p−ϕ_1'	ψ_1'	ω_1'	ϕ_2'	ψ_2'	ω_2'
I	80.9	173.4	119.1	−179.1	−58.2	−54.8	−179.7
II	96.3	−177.1	109.0	178.3	−69.0	−58.4	179.1
III	91.2	172.7	89.5	−175.3	−73.9	−28.3	179.4
IV	79.1	175.4	115.9	179.6	−50.1	−62.1	−168.6
VI	70.6	−153.8	102.7	−175.4	−48.0	−38.3	175.1

[a] See Figure 6 for a more detailed description of the torsion angles.

Table 8. Side Chain Angles in the Superimposed Conformations from Molecules **I**−**IV** and **VI**

	torsion angles[a] (deg)				
molecule	χ_{11}	χ_{12}	χ_{12}'	χ_{21}	χ_{22}
I	178.2	−178.8	59.6	−179.8	89.8
II	175.7	171.2	−66.8	−66.5	3.7
III	169.1	176.6	54.2	−97.4	52.0
IV	169.1	−179.7	57.9	(−71.3)	
VI	161.7	178.2	−59.8	−178.9	90.1

[a] See Figure 6 for a more detailed description of the torsion angles.

Two possible conclusions here are that (i) the pharmacophore modeling in this instance was incapable of suggesting the necessary stereochemistry of these cyclopropane compounds at P_1' for their HFC activity, or (ii) both isomers are bioactive. Later separation of the two diastereomers showed that both isomers were equally active.

Since in the CSD there were two basic conformations of trans nine-membered lactams with ψ angles −60° as used above and 145−150°, we rotated the ψ_2' angle of the rest of the molecules at 150° and evaluated the energies after minimization. This experiment suggested that ψ_2' at 150° is an equally possible torsion angle for the active conformation.

Molecular Dynamics Study of the Pharmacophore Geometry. The clustering information of the backbone torsion

Table 9. Clustering Information of the Backbone Torsion Angles of Molecules **I**–**V** in the 20 ps Trajectory Starting from the First Pharmacophoric Conformation at 300 K

molecule	torsion angles[a] (deg)						
	p−ω	p−ϕ_1'	ψ_1'	ω_1'	ϕ_2'	$\psi_2''^{b}$	ω_2'
I	80, 60, 100 (−16 ps); 270, 240, 300	−170, −200, −145 (20 ps)	120, 80, 150 (20 ps)	180, 160, 200 (20 ps)	−80, −120, −50 (16 ps); −160, −180, −140	−50, −20, −70 (14 ps); 95, 30, 160	180, 160, 200 (20 ps)
II	−40, −80, 0 (12 ps); 140, −110, 170 (4 ps); 40, 0, 80	180, 165, 195	160, 140, 180 (8 ps); −25, −50, 0 (12 ps)	180, 160, 200	−100, −135, −65	110, 40, 180 (12 ps); 3 rotations	180, 165, 195
III	80, 40, 120 (18 ps); 225, 175, 275 (4 ps)	−165, −190, −145	100, 80, 120	180, 165, 195	−80, −95, −65	−80, −95, 60	180, 160, 200
IV	80, 50, 110 (8 ps); −125, −160, −75	−175, −195, −150	100, 60, 150	180, 160, 200	−90, −45, −150 (8 ps); −300, −330, −270	−20, −45, 0 (4 ps); −80, −110, −55	−150, −175, −135
V	120, 80, 160 (8 ps); 285, 255, 315	140, 125, 155	100, 70, 140	180, 160, 200	−110, −150, −70	−60, −115, 0 (4 ps); 100, 40, 160	182, 205, 160

[a] The first three values are the average, lower, and upper ranges of the cluster. The value within parentheses is the approximate time period spent by the molecule in that cluster. Since the total simulation was for 20 ps, we did not record time information for the last cluster.

angles in the 20 ps trajectory at 300 K are given in Table 9, and the side chain torsion angles are summarized in Table 10. A few important aspects of these trajectories are summarized below:

(i) Most of the backbone torsion angles wagged around the pharmacophoric conformation, except torsion angles p−ω and ψ_2.

(ii) p−ω clustered around two conformations, one around 100° (the proposed pharmacophoric conformation), the other around −90°. However, the X-ray structure, as discussed later, differed from the proposed pharmacophoric conformation only in this torsion angle, and the X-ray value was −107°.

(iii) As in the pharmacophoric geometry, ψ_2 in the trajectory dynamics wagged around the same two angles for all molecules except **III** and **IV**. Here the torsion angle wagged around the starting angle −60°. The X-ray data indicated that this angle is around 132° (see the later part of this section). It is possible that the 20 ps trajectory at 300 K may not be sufficient for these conformational changes due to complications from the ring pucker in these two compounds.

NMR Constraints Found in the HFC-Bound Inhibitor. An ^{15}N-edited and decoupled NOESY spectrum of compound **VII** in the presence of HFC is displayed in Figure 9. The mixing time for this experiment is 100 ms. All the observed NOE peaks are due to distance constraints to the labeled NH in the inhibitor, either from within the inhibitor itself or from collagenase. The diagonal peak at 7.92 ppm is due to the collagenase-bound inhibitor, while that at 8.22 ppm is due to the free inhibitor. This spectrum demonstrated unambiguously that all of the NOE peaks derive from the labeled NH of the bound inhibitor.

In addition to the two cross peaks due to the two prochiral β protons (at 2.70 and 3.03 ppm) of the phenylalanine and one α proton peak (at 5.3 ppm), a methyl peak at 0.05 ppm is also observed. This peak can be detected with a mixing time as short as 45 ms (data not shown). Therefore, the methyl group must be within a short distance from the labeled NH, possibly less than 3 Å. As there is only one label in this compound, it is impossible to distinguish intermolecular and intramolecular NOEs. Therefore, the methyl group may be either from the protein or from the inhibitor. It is highly probable, however, that it is a sequential NOE from the isobutyl group of P_1' site. This observation was extremely helpful in identification of conformation of the P_1' isobutyl group in the pharmacophoric model. Since the terminal methyl groups of this side chain were not a part of the pharmacophoric atoms (see Figure 5), there were several low-energy conformations coming from the rotation of this group in the pharmacophoric grid that could be a possible conformation. The lowest energy conformation was selected arbitrarily. This conformation had a distance of 3.1 Å between the P_2' N and the nearest methyl H, in accord with the NMR data.

The horizontal slice of the NOESY spectrum at 7.92 ppm (Figure 9b) also shows clearly that the two prochiral β protons have strong and comparable NOE intensities. On the other hand, the cross peak with the phenylalanine ortho H's, possibly at 7.19 ppm, is very weak. These results suggest that the two β protons are at similar distances from the NH and the phenyl ring is probably in the trans position to it. This observation was consistent with the suggested active conformation of I, Table 6. A more extensive measurement of *J*-coupling constants confirms this picture and will be published in the near future.

Active Conformation in the X-ray Crystallographically Solved Structure. The structure of mature truncated collage-

Table 10. Approximate Clustering Information of the Side Chain Torsion Angles of Molecules **I**–**V** in the 20 ps Trajectory Starting from the First Pharmacophoric Experiment

molecule	torsion angles[a] (deg)			
	χ_{11}	χ_{12}	χ_{21}	χ_{22}
I	180, 160, 200 (20 ps)	185, 170, 200 (20 ps)	180, 160, 210 (20 ps)	70, 40, 100 (15 ps); −90, −120, −60
II	115, 105, 125	180, 155, 205	−60, −85, −35	−75, −110, −40 (14 ps); 95, 60, 130
III	185, 160, 220	190, 160, 220	−95, −110, −85 (19 ps); −115, −125, −105	60, 15, 110
IV	−175, −195, −155	−175, −195, −150	100, 85 120 (4 ps); 180, 160, 200	−65, −75, −40 (4 ps); −100, −115, −80
VI	205, 180, 230	187, 170, 210 (16 ps); 275, 255, 305	−55, −85, −30	105, 70, 135

[a] The first three values are the average, lower, and upper ranges of the cluster. The value within parentheses is the approximate time period spent by the molecule in that cluster. Since the total simulation was for 20 ps, we did not record time information for the last cluster.

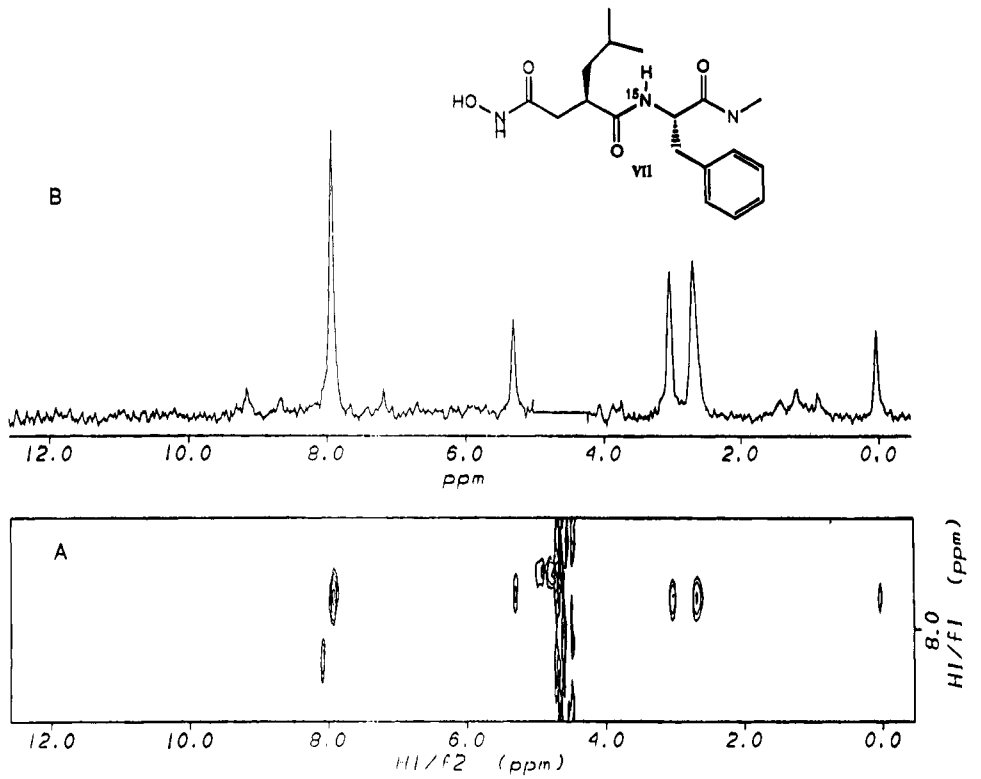

Figure 9. A ^{15}N-edited and decoupled NOESY spectrum of compound **VII** in the presence of 2.1 mM collagenase: (A) The 2D spectrum and (B) the horizontal 1 D slice through the 7.92 ppm diagonal peak, with residual water signal removed for display purposes.

Table 11. Comparison of the Computed Pharmacophore Model with the X-ray Structure of the Protein–Ligand Complex

angle name	pharmacophore model[a] (angle, deg)	X-ray	Δ(P−X)[c]
p−ω	91−129 (110)	253	153
p−ϕ_1	153−178 (166)	183	17
ψ_1	89−148 (120)	110	10
ω_1	177−185 (180)	191	11
ϕ_2	276−302 (293)	271	22
ψ_2	299−332 (307) [146][b]	132	14
ω_2	179−192 (183)	178	5
χ_{11}	169−185 (177)	190	13
χ_{12}	146−202 (176)	172	4
χ_{21}	180[d]	183	7
χ_{22}	90	73	17

[a] The angle range is given from the first experiment. The values within parentheses are the average values in different inhibitors. [b] The value suggested from the alternate conformation of trans nine-membered lactam in the Cambridge Structural Database. [c] The difference from the midpoint of the pharmacophore model range. [d] The value from the unconstrained acyclic compound **I** only. See the Results and Discussion section for more information about this torsion angle.

nase bound to the P_2' Phe analog of inhibitor **I** was recently solved in our laboratory.[22] The geometry of the ligand at the active site is given in Table 11. It is obvious from the comparison that all of the computed torsion angles are very close to these in the X-ray structure. The computed structure differed from the X-ray structure only at the p−ω torsion angle, where it differed by approximately 180°. This was not suprising, given the very low energy necessary to rotate this torsion angle. The χ_1 angle at the P_2' site in molecule **I** was found to be close to 180° in the pharmacophoric model. For other compounds it was constrained by the ring structure, or the lowest energy conformation had a different angle (χ_{21} in Table 6 and 8). Fair activity of most of these compounds suggested that this angle probably was not critical for the activity. The X-ray crystal structures of several HFC and other collagenase ligands have recently been completed[43,44] and favored this conclusion. This distance of one of the P_1' methyl groups from the P_2' N was 3.3 Å, favoring the pharmacophore model as well as the NOE data.

(43) Lovejoy, B.; Cleasby, A.; Hassell, A. M.; Longley, K.; Luther, M. A.; Weigl, D.; McGeehan, G.; McElroy, A. B.; Drewry, D.; Lambert, M. H.; Jordan, S. R. *Science* **1993**, *263*, 375–377.

(44) Borkakoti, N.; Winkler, F. K.; Williams, D. H.; D'Arcy, A.; Broadhurst, M. J.; Brown, P. A.; Johnson, W. H.; Murray, E. J. *Nat. Struct. Biol.* **1994**, *1*, 106–110.

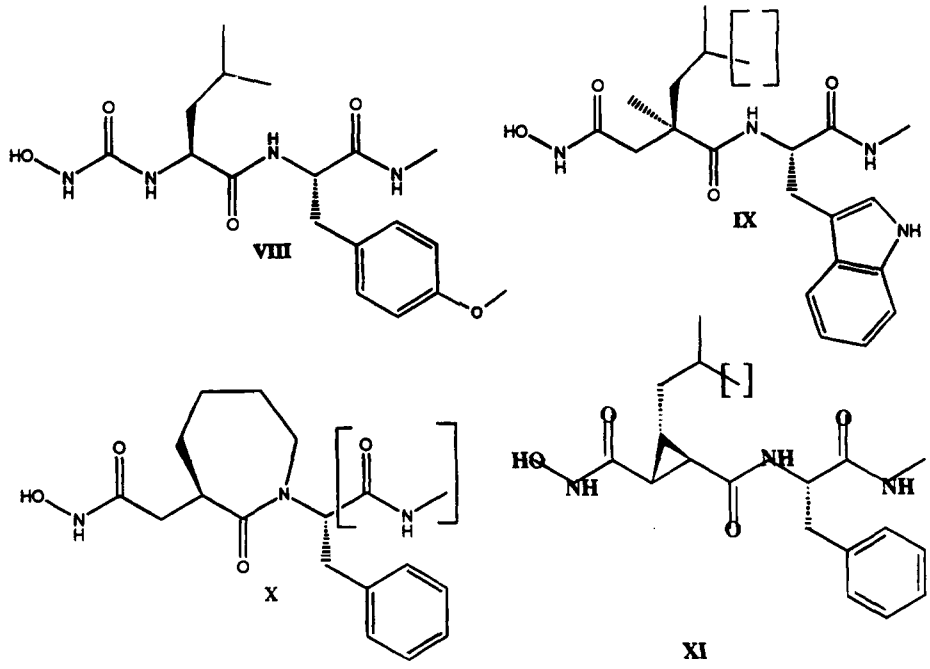

Figure 10. A few compounds whose activities were rationalized from the pharmacophoric model. The structural moiety within [ ] were envisioned at the early stage but not synthesized. See descriptions in Results and Discussion for details.

Application of the Model in the Drug Design Problem. One major application of a pharmacophore model may be as an aid in the quantitative interpretation of the binding affinity data, specifically, by developing a 3D-QSAR model.[4,45-49] The initial step of all these methods is to align the molecules in three-dimensional space. However, such developments need a considerable variation in the physicochemical parameters around the molecule. Since the current available data set did not have enough physicochemical diversity, the pharmacophore model was used qualitatively. The qualitative approach used three basic criteria: (i) In order to be an active compound, a test molecule should be able to orient the pharmacophoric groups in the proposed active conformation. (ii) This conformation should be a low-energy conformation. (iii) If any part of the test molecule in its active conformation occupies a region unoccupied by the known active compounds, one should be skeptical about its inhibition potency.

The first criterion can be checked using any distance-constrained conformational search technique. However, one cannot accept this conformation as a low-energy conformation without knowing the energy of the global minimum energy conformation. We found that a modified pattern search technique as described before[9,50] was extremely useful for the energetic evaluation of an acceptable conformation. In this method each torsion angle is rotated within its nonrepeating domain starting from the acceptable conformation with a specified increment and is fixed at the minimum energy angle before proceeding to the next torsion angle. The process is continued sequentially for all rotatable torsion angles and iteratively until it converges. If the energy decrease in this process is small, the conformation can be accepted with a considerable confidence.

The most remarkable prediction of this study was the activity of diastereomeric cyclopropane derivatives **V** and **VI**. However, we will discuss a few interesting compounds (Figure 10) whose activity could be rationalized using the pharmacophoric model and the above mentioned guidelines. The hydroxyurea **VIII** showed poor activity against HFC. It could not attain the pharmacophoric arrangement, since the p$-\omega$ torsion angle in **VIII** is planar, while that in the active conformation was $-107°$. In compound **IX** (K_i = 0.63 μM), a methyl analog of **I**, the active conformation could be attained in a low-energy conformation. However, the extra methyl group occupied a region unoccupied in any other active compounds. This is also consistent with the X-ray crystallographic structure.[22] This region is blocked by PRO-238. In the pharmacophoric model as well as in the X-ray active conformation, one of the methyl groups of the isobutyl group of P_1' Leu was close to the P_2' NH. Since cyclization helps the free energy change (ΔG) of binding by increasing the ΔS, the compound **X** was envisioned as a good target. However, the necessary active conformation here is a boat-like conformation, and the actual crystallographic conformation is a chair-type conformation (ref codes BAJZOB10, BILJOV, CAPLAC, CAPLAC01, DIKVAU, DOKMUL, and VIMXYI in the Cambridge Crystallographic Database[38]). The molecular mechanics energy difference between the boat and the chair conformation of the simplest lactam was found to be between 4 and 5 kcal/mol, depending on the force field used. This negated the anticipated gain in binding. The synthesis of **X** was abandoned after the phenethyl derivative (lacking the P_2' carboxamide) showed poor activity compared to that of comparable compounds from several other active analogs. On the other hand, compound **XI** was originally modeled with the isobutyl moved one carbon in the cyclopropyl ring. That compound needed more than 6 kcal/mol energy to attain the active conformation. The problem seemed to be due to a bad steric interaction between one of the methyl groups and the hydroxamate group. Removal of one of the methyl groups showed that the active conformation can be attained at the cost of approximately 3.5 kcal/mol, and this compound showed fair activity against HFC (0.2 μM).

(45) Hopfinger, A. J. *J. Am. Chem. Soc.* **1980**, *102*, 7196-7206.
(46) Ghose, A. K.; Crippen, G. M. *J. Med. Chem.* **1984**, *27*, 901-914.
(47) Ghose, A. K.; Crippen, G. M. *J. Med. Chem.* **1985**, *28*, 333-346.
(48) Cramer, R. D.; Patterson, D. E.; Bunce, J. D. *J. Am. Chem. Soc.* **1988**, *110*, 5959-5967.
(49) DePriest, S. A.; Mayer, D.; Naylor, C. B.; Marshall, G. R. *J. Am. Chem. Soc.* **1993**, *115*, 5372-5384.
(50) Jaeger, E. P.; Peterson, M. L.; Treasurywala, A. M. *J. Comput.-Aided Mol. Des.*, submitted.

Critical Comments and Conclusion

The present analysis technique of the orientation map allows one to extract the best available superimposable conformation, independent of the grid size used.

Unlike the distance geometry or ensembled distance geometry solution, a limit can be easily imposed on the energy of the evaluated conformation.

This work has clearly indicated that a pharmacophore model can reliably be built using the distance information of the low-energy conformations of a series of conformationally diverse active ligands.

Even individual dynamics starting from the proposed bioactive conformation may shed some light on a few possible alternative conformations close to the starting conformation.

When one or more torsion angles are constrained by a ring, the alternate possible conformations of the ring should be considered as possible solutions.

An NMR study of the enzyme-bound isotopically labeled ligand can be a valuable tool for verifying or suggesting the active conformation.

One may, however, be critical about a few aspects of the method. Constraining the conformation often leads to a loss of binding affinity, although the entropy factor arising from the conformational distribution should help the binding. The problem in these chosen molecules may be due to fixation of the conformation at an angle somewhat distant from the ideal angle or due to a bad interaction of the constraining part with the enzyme binding site. It is not certain how much drop in activity of a molecule should be acceptable in this type of modeling. The idea of pharmacophoric modeling does not hold if the inhibitors show considerable activity even when one or more pharmacophoric groups do not reach the same region of the active site. Forcing the molecules to attain a conformation where equivalent groups occupy the same location in such a situation may give a distorted pharmacophoric model. However, the success in the drug design process is so rare that the researchers in this area are often eager to take these risks. The only suggestion to be offered here may be to analyze the suggested (computed) conformation with the existing knowledge of conformation of similar molecules.

Acknowledgment. The authors want to thank Drs. R. Goswami and R. McGarry of Eastman Kodak Co. for allowing them to use one of their compounds (**III**) in this paper, and B. Murray, R. Olyslager, and J. Seelye for synthetic assistance.

JA942244N